Title

Urotensin 2 in Kawasaki disease pathogenesis

Journal

Pediatric Research, 82(6)

ISSN

0031-3998

Authors

Huang, Cassidy Y
Burns, Jane C
Shimizu, Chisato

Publication Date

2017-12-01

DOI

10.1038/pr.2017.183

Peer reviewed

nature publishing group

Urotensin 2 in Kawasaki disease pathogenesis

Cassidy Y. Huang[1], Jane C. Burns[1] and Chisato Shimizu[1]

BACKGROUND: Genetic variation in calcium signaling pathways is associated with Kawasaki disease (KD) susceptibility and coronary artery aneurysms (CAA). Expression quantitative trait locus analysis for KD-associated variants in calcium/sodium channel gene solute carrier family 8 member 1 (SLC8A1) revealed an effect on expression of urotensin 2 (UTS2). We speculated that UTS2 is influenced by genetic variation in SLC8A1 and contributes to disease pathogenesis.
METHODS: We measured levels of UTS2 and its receptor in blood and tissues using quantitative reverse transcription-polymerase chain reaction, enzyme-linked immunosorbent assay, and immunohistochemical staining.
RESULTS: UTS2 transcript levels were higher in the whole blood of subjects with KD homozygous for three risk alleles in SLC8A1 ($P = 0.002$–0.006). Increased levels of plasma UTS2 varied as a function of SLC8A1 genotype ($P = 0.008$–0.04). UTS2 and UTS2 receptor were expressed in mononuclear inflammatory cells and spindle-shaped cells in the coronary arterial wall of a patient suffering from KD with CAA and in a femoral endarterectomy specimen from an adult patient with peripheral aneurysms following KD in childhood.
CONCLUSION: Host genetics influences UTS2 levels, which may contribute to inflammation and cardiovascular damage in KD.

Kawasaki disease (KD) is an acute, self-limited vasculitis of the systemic, medium-sized arteries (1). Without treatment, about 25% of patients suffering from KD develop coronary artery aneurysms (CAA), making it the most common cause of acquired heart disease in children in developed countries (2). Although the acute febrile illness is self-limited, the formation of CAA and ongoing tissue inflammation result in long-term morbidity (3). The exact mechanism of CAA formation in patients suffering from KD has not been elucidated. However, evidence suggests that myofibroblast-like cells mediate damage to the arterial wall and may have an important role in aneurysm formation (4). Other complications of KD include aneurysms in systemic arteries and cardiac sequelae including cardiac fibrosis (3,5,6).

Although the etiology of KD is unknown, previous epidemiologic studies suggest that host genetics influences KD susceptibility (7,8). Recently, we reported three single-nucleotide polymorphisms that are in linkage disequilibrium ($r^2 = 0.56$–0.93) in the gene solute carrier family 8 member 1 (SLC8A1: rs10490051, rs13017968, and rs12989852) and that are associated with KD susceptibility and CAA (9). Expression quantitative trait loci (eQTL) analysis was performed on one of the three SLC8A1 variants (rs13017968), which was found to influence the expression of urotensin 2 (UTS2).

UTS2 is an 11 amino acid cyclic peptide expressed in monocytes, endothelial cells, vascular smooth muscle cells, and fibroblasts. It has diverse effects upon binding to the urotensin 2 receptor (UTS2R), including potent vasoconstriction mediated by vascular smooth muscle cells (VSMCs), proliferation of VSMCs and fibroblasts, and chemotaxis of inflammatory cells (10,11). UTS2 increases expression of monocyte-chemoattractant protein-1 (MCP-1), a chemoattractant for monocytes that was previously reported to be elevated in patients with KD (12–14). UTS2 itself is a chemoattractant for monocytes that express the UTS2R (15). UTS2 has also been associated with myocardial and cardiac fibrosis (16,17). However, the role of UTS2 in KD has not been previously investigated. In the present study, we speculated that subjects with KD homozygous for SLC8A1 risk alleles have increased UTS2 expression, which contributes to inflammation and cardiovascular damage. We tested the hypothesis by studying UTS2 transcript levels in blood, as well as UTS2 and UTS2R protein concentrations in blood and their distribution in tissues from patients with KD.

METHODS

Subjects

Two subject cohorts were used for three different analyses. Cohort 1 ($n = 146$) comprised subjects for whom we had previously published transcriptome data and cohort 2 ($n = 30$) was an independent cohort used to validate the transcript abundance data from cohort 1 and to measure protein levels of the molecules of interest. The demographic and clinical characteristics of the 30 subjects with KD (cohort 2) are presented in Table 1. The subjects were grouped by the SLC8A1 genotype for the three risk alleles and the data are presented in **Supplementary Table S1** (rs10490051), **Supplementary Table S2** (rs13017968), and **Supplementary Table S3** (rs12989852). Allele frequencies for the three SLC8A1 risk loci single-nucleotide polymorphisms (rs10490051, rs13017968, and rs12989852) are presented in **Supplementary Table S4** for both the independent cohort of subjects suffering from KD (cohort 2) and for control subjects from the 1000 Genomes database. All subjects met the American Heart Association (AHA) criteria for KD. The variable *z*-worst is the maximal standard deviation units from the mean (*z*-

[1]Department of Pediatrics, University of California, San Diego School of Medicine, La Jolla, California. Correspondence: Chisato Shimizu (c1shimizu@ucsd.edu)

Received 3 March 2017; accepted 13 July 2017; advance online publication 16 August 2017. doi:10.1038/pr.2017.183

Table 1. Demographic and clinical characteristics of subjects with KD used for qRT-PCR and ELISA

	KD patients ($n = 30$)
Age	2.1 (1.3–3.7)
Males, *n* (%)	19 (63)
Ethnicity	
Asian, *n* (%)	8 (27)
Caucasian, *n* (%)	5 (17)
Native American, *n* (%)	1 (3)
Hispanic, *n* (%)	11 (37)
Mixed, *n* (%)	5 (16)
Illness day, median (range)[a]	5 (2–11)
Coronary artery status	
Aneurysm, *n* (%)	3 (10)
Dilated, *n* (%)	11 (37)
Normal, *n* (%)	16 (53)
z-Score, median (range)[a]	2.1 (0.5–5.2)
Lab data	
WBC (10^3/μl)	13.5 (11.1–15.5)
Polys (%)	54 (47–62)
Lymphocytes (%)	25 (20–34)
Monocytes (%)	5 (2–9)
Eosinophils (%)	2 (1–4)
Absolute band count	1,024 (504–1,883)
Absolute neutrophil count	8,917 (6,308–10,359)
Hemoglobin (mg/dl)	11 (10.3–11.5)
Z-hemoglobin[b]	−1.5 (−2.4 to −0.7)
Hematocrit (%)	31.7 (31–34)
Platelets (10^3/mm^3)	378 (289–458)
ESR (mm/h)	57.5 (43–70)
CRP (mg/dl)	6.2 (4.1–11.8)
ALT (iu/l)	47.5 (30.2–86.5)
GGT (iu/l)	42 (20–89)

ALT, alanine aminotransferase; CRP, C-reactive protein; ESR, erythrocyte sedimentation rate; GGT, gamma-glutamyl transferase; Polys, polymorphonuclear cells; WBC, white blood count.
[a]All data are represented as a median (interquartile range) unless otherwise specified.
[b]*Z*-hemoglobin is the hemoglobin concentration normalized for age and expressed as standard deviation units.

score) measurement of the internal diameters in mm of the proximal right coronary arteries and left anterior descending coronary arteries normalized for body surface area. Dilatation of the coronary arteries was defined as a *z*-score of ≥ 2.5, CAA was defined as a *z*-score of ≥ 4, and giant CAA was defined as a *z*-score of ≥ 10. Laboratory data were obtained during the acute phase before intravenous-immunoglobulin (IVIG) administration. Parental informed consent and patient assent were obtained from all subjects. The study protocol was reviewed and approved by the University of California, San Diego Institutional Review Board.

Sample Collection and RNA Extraction

EDTA plasma was collected in tubes containing sodium EDTA during the acute phase before IVIG administration, and processed within 48 h of sample collection. Peripheral blood mononuclear cells were collected in tubes containing sodium heparin and isolated by density gradient centrifugation using Histopaque (Sigma Aldrich, St. Louis, MO) within 48 h of sample collection. The plasma samples were stored at −80 °C until use. Whole blood was collected in PAXgene tubes (PreAnalytiX, Homebrechtikon, Switzerland) during the acute phase before IVIG administration. PAXgene tubes were frozen at −20 °C until RNA extraction. RNA extraction was performed using PAXgene blood mRNA kit (Qiagen, Hilden, Germany) according to manufacturer's instructions.

Tissue Samples and Histology

Formalin-fixed, paraffin-embedded tissues were obtained from two subjects with a history of KD, and one control patient. Tissues for case 1 were obtained at the time of autopsy and tissues for case 2 were obtained at the time of surgery. The demographic and clinical characteristics of case 1, case 2, and the control are presented in Table 2. The complete clinical course of cases 1 and case 2 was previously published (5,6,18). Informed consent was obtained from the subjects or their parents. Histochemical staining with Masson trichrome stains was performed using standard techniques.

Microarray Analysis

UTS2 transcript levels in the whole blood of 131 paired acute and convalescent subjects with KD were analyzed using a published microarray data set (19). Microarray probe location was indicated in **Supplementary Figure S1**. The demographic and acute clinical characteristics of the subjects used for the microarray analysis are presented in Table 3. **Supplementary Table S5** (rs10490051), **Supplementary Table S6** (rs13017968), and **Supplementary Table S7** (rs12989852) show the characteristics grouped by SLC8A1 risk loci.

Genotyping

Genomic DNA was extracted from the whole blood using Wizard Genomic DNA purification kit (Promega, Madison, WI), or from formalin-fixed, paraffin-embedded tissues using QIAamp DNA FFPE tissue kit (Qiagen, Hilden, Germany). The subjects with KD were genotyped by PCR for SLC8A1 rs10490051, rs13017968, and rs12989852 (Life Technologies, Waltham, MA).

Quantitative Reverse Transcription-Polymerase Chain Reaction Validation of Microarray Results

To validate published microarray results showing differential UTS2 expression by SLC8A1 genotype, UTS2 transcript levels for an independent cohort of 30 subjects with KD were measured by quantitative reverse transcription-polymerase chain reaction (qRT-PCR). cDNA was made from whole-blood RNA collected in PAXgene tubes (SuperScript III reverse transcriptase, ThermoFischer, Waltham, MA). qRT-PCR was performed according to the manufacturer's instructions using commercially available UTS2 Taqman primers (ThermoFischer). The Taqman PCR product location is shown in **Supplementary Figure S1**. The relative abundance of UTS2 transcripts was normalized to the expression levels of TATA box binding protein-associated factor, RNA polymerase I, B (TAF1B) (Life Technologies).

Plasma UTS2 and MCP-1 Measurement Using ELISA

Plasma UTS2 and MCP-1 levels were measured by ELISA according to the manufacturer's instructions (UTS2: Phoenix Pharmaceuticals, Burlingame, CA, and MCP-1: R&D Systems, Minneapolis, MN).

Table 2. Demographic and clinical characteristics of subjects with KD and control subjects for immunochemical staining

Case	Age/sex	Ethnicity	Age of KD onset	Procedure	Clinical course	Tissues obtained
1	15 months/M	Caucasian	5 months	Autopsy	Giant aneurysm at KD onset at 5 months. Death due to cardiac arrest from thrombotic occlusion of giant aneurysm	Coronary artery
2	31 years/M	Caucasian	7 weeks	Left iliac endarterectomy	CAA and bilateral axillary aneurysms at KD onset. Developed right lower extremity claudication at age 22 and age 25. At age 30, both femoral arteries were diseased with stenosis. Left iliac artery had thickened intima with diffuse fibrosis and calcification.	Intima of femoral artery
Control	4 years/F	N/A	N/A	Autopsy	Congenital diaphragmatic hernia	Coronary artery/ myocardium

CAA, coronary artery aneurysms; KD, Kawasaki disease; N/A, not available.

Table 3. Demographic and clinical characteristics of subjects with KD in microarray data set

	KD patients ($n = 131$)
Age	2.7 (1.4–4.1)
Males, *n* (%)	80 (61)
Ethnicity	
Asian, *n* (%)	22 (17)
African American, *n* (%)	5 (4)
Caucasian, *n* (%)	35 (27)
Hispanic, *n* (%)	32 (24)
Mixed, *n* (%)	37 (28)
Illness day, median (range)[a]	6 (2–11)
Coronary artery status	
Aneurysm, *n* (%)	12 (9)
Dilated, *n* (%)	29 (22)
Normal, *n* (%)	90 (69)
Z-worst, median (range)[a]	1.8 (0.2–18.3)
Lab data	
WBC (10^3/μl)	13.6 (11–19)
Polys (%)	54 (42–63)
Lymphocytes (%)	21 (13–31)
Monocytes (%)	6 (4–8)
Eosinophils (%)	2 (0–3)
Absolute band count	1,771 (456–2,820)
Absolute neutrophil count	9,027 (6,780–12,390)
Hemoglobin (mg/dl)	11.3 (10.5–11.8)
Z-hemoglobin[b]	−1.5 (−1.9 to −0.4)
Hematocrit (%)	32.8 (31–34)
Platelets (10^3/mm^3)	412 (321–475)
ESR (mm/h)	61 (44–82)
CRP (mg/dl)	8 (4.6–16.4)
ALT (iu/l)	33 (17–109)
GGT (iu/l)	30 (17–93)

ALT, alanine aminotransferase; CRP, C-reactive protein; ESR, erythrocyte sedimentation rate; GGT, gamma-glutamyl transferase; Polys, polymorphonuclear cells; WBC, white blood count.
[a]All data are represented as a median (interquartile range) unless otherwise specified.
[b]*Z*-hemoglobin is the hemoglobin concentration normalized for age and expressed as standard deviation units.

Immunochemical Staining of Tissues

Tissues were fixed in formalin and embedded in paraffin. The tissue sections were deparaffinized and rehydrated using standard methods. Endogenous peroxidase activity was quenched with 3% hydrogen peroxide (Abcam, Cambridge, MA). Antigen retrieval was performed using citrate buffer in a microwave for 10 min. Nonspecific binding was blocked using milk in PBS for 10 min (Abcam). Slides were incubated with primary antibodies, anti-human UTS2 rabbit polyclonal antibody, anti-human UTS2R rabbit polyclonal antibody,

and anti-human CD14 (Novus Biologicals, Littleton, CO, 1:100 dilution and 1:100 dilution, and Biolegend, San Diego, CA, respectively), at 4 °C overnight. Rabbit IgG was used as the primary antibody for the negative-staining controls (Dako, Carpinteria, CA). Bound primary antibodies were detected using a biotinylated secondary antibody, enzyme-labeled streptavidin, and visualized by substrate-chromogen (Abcam).

Statistical Analysis

Data were analyzed using GraphPad Prism (GraphPad Software, La Jolla, CA). Mann–Whitney *U* test and the Kruskal–Wallis test were used to compare continuous variables. Correlation coefficients were calculated using the Pearson correlation coefficient test. Chi-square test was used to compare equality of proportions. Two-tailed *P*-value <0.05 was considered statistically significant.

RESULTS

UTS2 Transcript and Protein Levels

Using a KD microarray data set from paired acute and convalescent whole-blood samples (cohort 1), we determined that subjects with KD homozygous for any of the three risk alleles in SLC8A1 (rs10490051, rs10317968, and rs12989852) had higher UTS2 transcript levels (**Supplementary Figures S2** and **S3**). The effect of the risk alleles on UTS2 expression in the acute phase was validated using qRT-PCR in whole blood collected pre-treatment from an independent cohort of 30 subjects with KD (cohort 2), with higher UTS2 transcript levels in risk allele carriers (**Figure 1**). However, no relationship was found between the risk alleles and expression of the receptor, UTS2R (data not shown). Next, we determined whether UTS2 plasma protein levels varied as a function of SLC8A1 genotype. Plasma UTS2 levels were higher in subjects with KD homozygous for the three risk alleles (**Figure 2**).

To determine whether UTS2 and UTS2R are differentially expressed as a function of patient characteristics and disease outcome, we analyzed whole-blood UTS2 transcript levels in 131 paired acute and convalescent subjects with KD (19). UTS2 transcript levels were significantly lower in the convalescent phase in subjects with KD with normal and dilated coronary arteries ($P=0.0001$ and $P=0.004$, respectively) (**Figure 3a,b**). Demographic and clinical factors except for ethnicity were similar among subjects with KD with different SLC8A1 genotypes (**Supplementary Tables S5–S7**). However, subjects with self-declared Asian ancestry were more likely to be homozygous for all three risk alleles. This is consistent with data from the 1000 Genomes database that show individuals of Asian descent having a higher allele frequency for the SLC8A1 risk alleles (**Supplementary Table S4**). No correlation was observed between UTS2 transcript levels and sex, illness day, age, coronary artery *z*-score, and the percentage of lymphocytes and monocytes in the whole blood of those subjects with KD (**Supplementary Figure S4**). In the subject who was wild-type homozygous for all three single-nucleotide polymorphisms, UTS2 transcript levels were undetectable when compared with the levels in the risk allele carriers.

UTS2R was not differentially expressed as a function of KD disease status or coronary artery status (**Supplementary Figure S5**). As UTS2R expression in blood was reported to be highest in monocytes (15), we analyzed the correlation

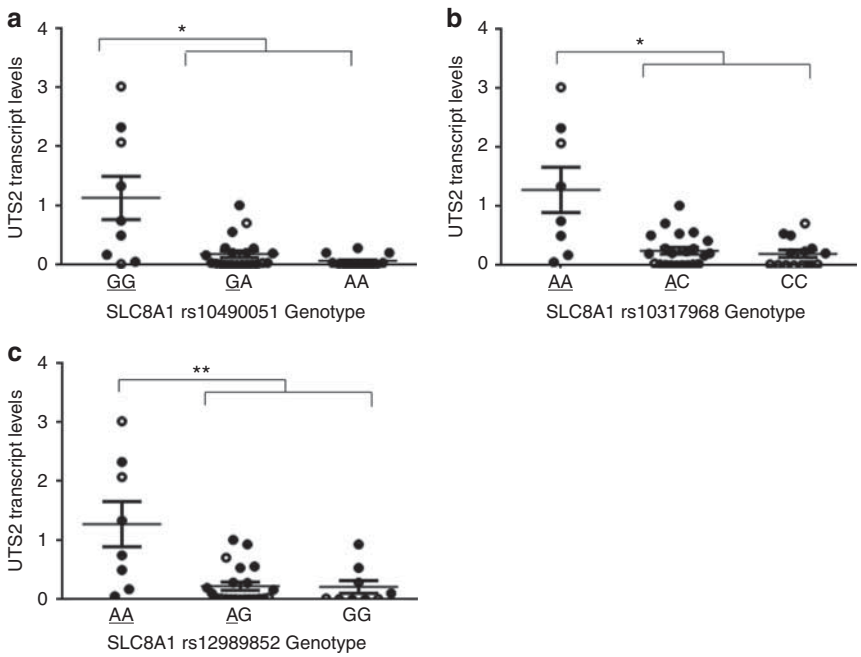

Figure 1. Differential expression of urotensin 2 (UTS2) as a function of solute carrier family 8 member 1 (SLC8A1) genotype by quantitative reverse transcription-polymerase chain reaction (qRT-PCR). Acute UTS2 transcript levels in whole blood of subjects with Kawasaki disease (KD) were stratified by (**a**) rs10490051 genotypes GG ($n=9$), GA ($n=9$), and AA ($n=12$), (**b**) rs13017968 genotype AA ($n=8$), AC ($n=8$), and CC ($n=14$), and (**c**) rs12989852 genotypes AA ($n=8$), AG ($n=13$), and GG ($n=9$). Risk alleles are underlined. *$P<0.05$; **$P<0.005$ for homozygous risk allele vs. all others.

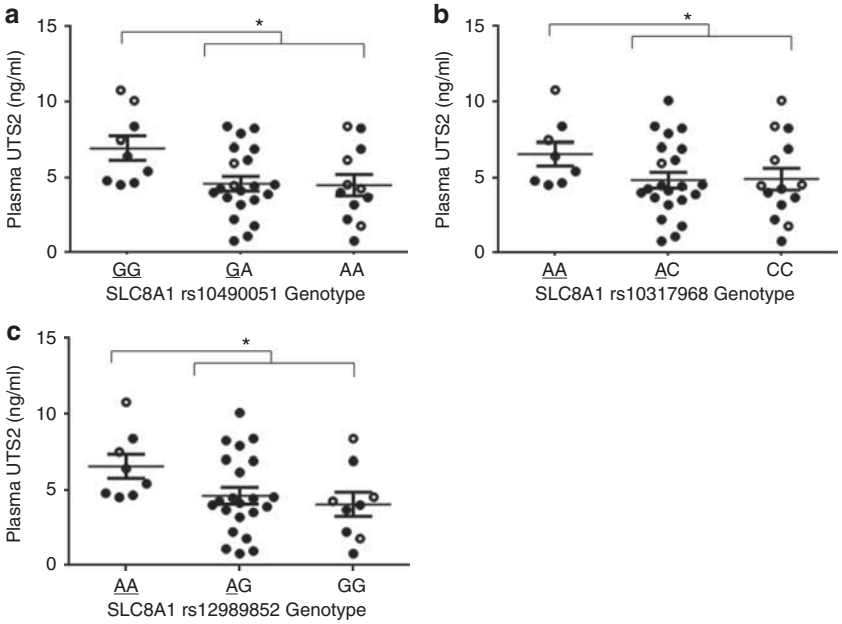

Figure 2. Plasma urotensin 2 (UTS2) levels (ng/ml) as a function of solute carrier family 8 member 1 (SLC8A1) genotype. Acute plasma UTS2 levels from subjects with KD were stratified by (**a**) rs10490051 genotypes GG ($n=9$), GA ($n=9$), and AA ($n=12$), (**b**) rs13017968 genotype AA ($n=8$), AC ($n=8$), and CC ($n=14$), and (**c**) rs12989852 genotypes AA ($n=8$), AG ($n=13$), and GG ($n=9$). Risk alleles are underlined. *$P<0.05$ for homozygous risk allele vs. all others.

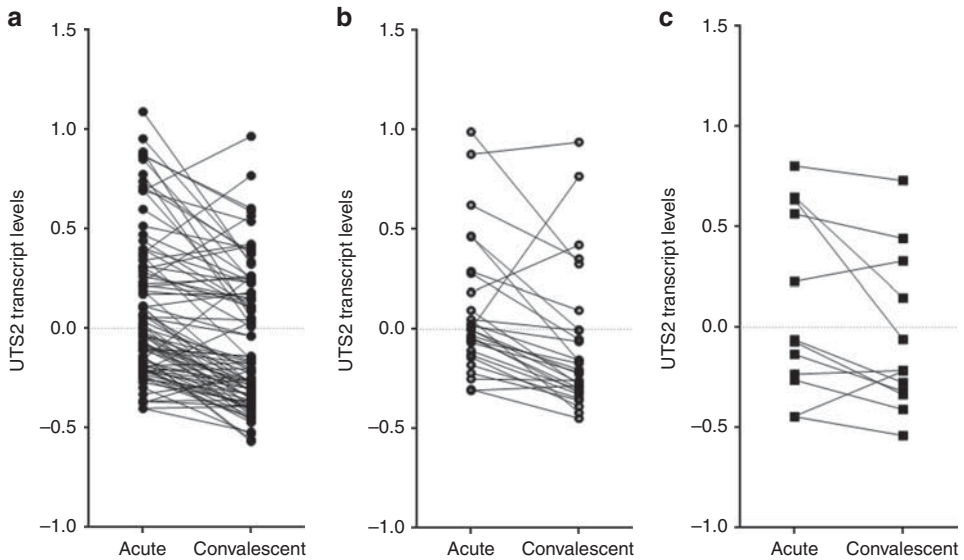

Figure 3. Urotensin 2 (UTS2) transcript levels as a function of coronary artery status. UTS2 transcript levels in whole blood were analyzed for paired acute and convalescent subjects with Kawasaki disease (KD): (**a**) Normal coronary arteries (left panel) ($n=90$) ($P=0.0001$) (**b**) dilated coronary arteries (middle panel) ($n=29$) ($P=0.004$), and (**c**) coronary artery aneurysms (right panel) ($n=12$) (not significant).

between the absolute number of monocytes and UTS2R transcript levels in whole blood, but no correlation was found (**Supplementary Figure S6**).

Plasma MCP-1 Levels as a Function of SLC8A1 Genotype

Since UTS2 induces MCP-1 secretion in rat adventitial fibroblasts (12), and in the present study, we showed that UTS2 transcript and protein levels are influenced by SLC8A1 genotype. Next, we determined whether SLC8A1 genotype influences MCP-1 secretion. Plasma MCP-1 levels (pg/ml) did not differ as a function of SLC8A1 genotype for any of the three SLC8A1 risk alleles (**Supplementary Figure S7**). Similarly, there was no correlation between UTS2 and MCP-1 levels in acute plasma samples (data not shown).

UTS2 and UTS2R Expression in Tissues

To understand the relationship between the UTS2/UTS2R axis and inflammation of the coronary arteries, we performed

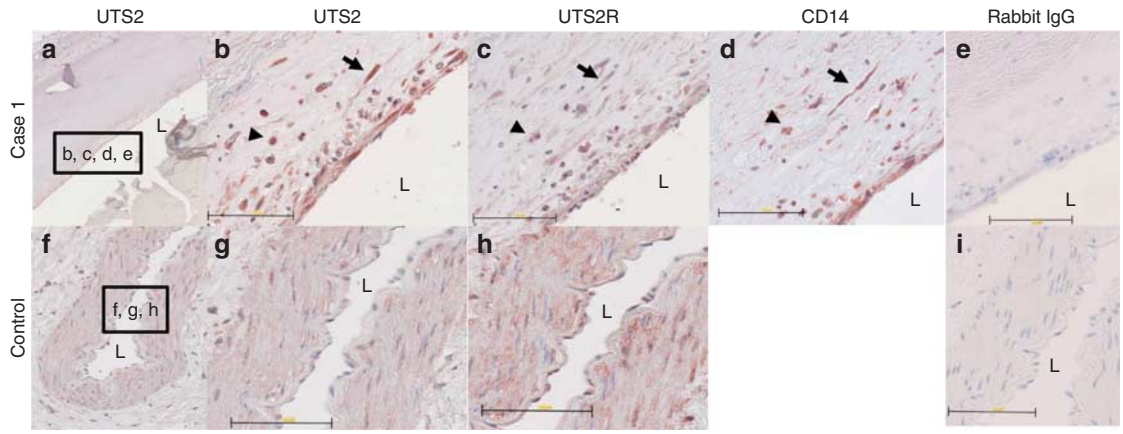

Figure 4. Urotensin 2 (UTS2) and urotensin 2 receptor (UTS2R) expression in the coronary artery of a subject with Kawasaki disease (KD) who died 10 months after the onset of KD. The coronary artery of case 1 was stained for (**a**) UTS2 at ×40, with boxed area indicating location of **b–e**, (**b**) UTS2, ×400, (**c**) UTS2R, ×400, (**d**) CD14+, ×400, and (**e**) rabbit IgG as a negative-staining control at ×400. The control coronary artery was stained for (**f**) UTS2, ×40, with boxed area indicating location of **g–i**, (**g**) UTS2, ×400, (**h**) UTS2R, ×400, (**i**) rabbit IgG, ×400. Arrows indicate spindle-shaped cells and arrowheads indicate mononuclear inflammatory cells in thickened intima. L, lumen. Bar = 100 μm.

immunochemical staining for UTS2 and UTS2R in the coronary artery of case 1, a patient suffering from KD with CAA who died 10 months after the onset of the disease. The artery had a giant aneurysm with thrombotic occlusion of the lumen, with destruction of the internal elastic lamina and thickening of the intima (**Figure 4a**). In the thickened intima, UTS2-, UTS2R-, and CD14-positive mononuclear inflammatory cells were present (**Figure 4b–d**, arrowheads), as well as spindle-shaped cells (arrows). The SLC8A1 genotype of case 1 could not be determined due to the poor quality of the DNA. The normal control coronary artery showed positive staining for UTS2 and UTS2R in endothelial cells and vascular smooth muscle cells (VSMC) (**Figure 4g,h**). No spindle-shaped cells or inflammatory cells were observed in the normal coronary artery.

To understand the possible relationship between the UTS2/UTS2R axis and vascular fibrosis in KD, we performed immunochemical staining for UTS2 and UTS2R in an endarterectomy specimen surgically resected from the femoral artery of case 2, an adult patient suffering from KD with vascular fibrosis (6). At 3 months of life, case 2 developed giant CAA and bilateral common femoral artery aneurysms. At 30 years of age, he developed claudication from stenosis of the common femoral artery bilaterally, and an endarterectomy was performed. Case 2 was homozygous for the risk alleles in SLC8A1 rs13017968, and heterozygous for the other two single-nucleotide polymorphisms. Masson's trichrome stain showed collagen deposition in the intima of the iliac artery (**Figure 5a**). Abundant UTS2- and UTS2R-positive spindle-shaped cells were noted on the luminal side of the thickened intima, where collagen deposition was also observed (**Figure 5b,c**, arrows).

DISCUSSION

In this study, we show that polymorphisms associated with KD susceptibility in SLC8A1, located on Chromosome 2, influence in *trans* the transcript abundance and protein expression of UTS2 on Chromosome 1. We have recently established the influence of SLC8A1 polymorphisms on susceptibility to KD and the risk of coronary artery abnormalities (9). Using our KD microarray database, we showed that SLC8A1 genotype can influence expression of UTS2 transcripts in whole blood, with the highest UTS2 transcript abundance in subjects homozygous for the SLC8A1 risk alleles. In an independent cohort, we confirmed that subjects with KD homozygous for all three risk alleles have increased UTS2 transcript levels and plasma protein levels. UTS2 and UTS2R were expressed in inflammatory cells and spindle-shaped cells with a myofibroblast-like morphology in the coronary artery. UTS2 and UTS2R were also expressed in spindle-shaped cells in an endarterectomy specimen from a remodeled aneurysm in the femoral artery following KD. These data suggest a possible role for UTS2 and UTS2R in vascular inflammation, aneurysm formation, and arterial remodeling.

The recruitment of monocytes to the arterial wall during acute KD could contribute to vessel wall inflammation and aneurysm formation. The exact mechanism of CAA formation in KD has yet to be clarified, but evidence suggests that monocytes and MCP-1, a chemoattractant for monocytes, are involved in the process (20,21). Monocytes were demonstrated to be more abundant during acute KD, particularly the CD14+CD16+ subpopulation (22). Studies conducted by Zhang *et al* (12) determined that UTS2, by binding UTS2R, increases expression and secretion of MCP-1 in rat aorta adventitial fibroblasts. Segain *et al.* (15) reported high UTS2R expression in CD14+CD16+ monocytes, and that UTS2 is a chemoattractant for monocytes that express UTS2R. UTS2 mRNA is most abundantly expressed in classical monocytes that are CD14+CD16− (23). Although increased plasma UTS2 levels did not correlate with increased plasma MCP-1 levels, UTS2 may have a role in monocyte chemotaxis in the

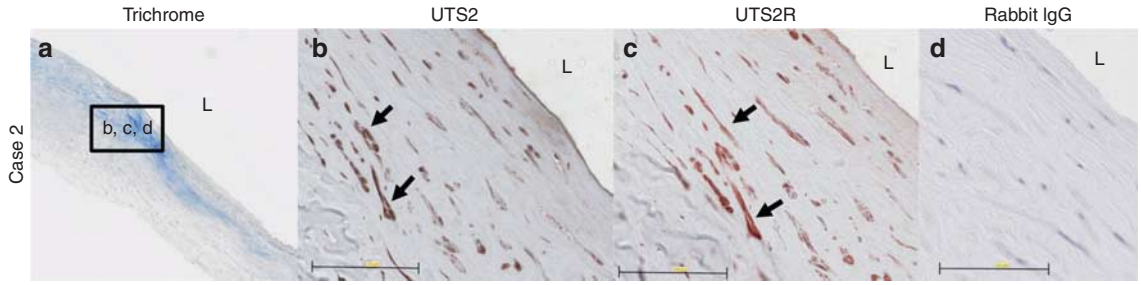

Figure 5. Urotensin 2 (UTS2) and urotensin 2 receptor (UTS2R) expression in an endarterectomy specimen of the femoral artery surgically removed from an adult subject with a history of Kawasaki disease (KD) complicated by coronary artery aneurysms (CAA) and femoral artery aneurysms. (**a**) Trichrome staining, ×40, with boxed area indicating location of **b–d**, (**b**) UTS2, ×400, (**c**) UTS2R, ×400, and (**d**) rabbit IgG as a negative-staining control, ×400. Arrows indicate spindle-shaped cells. L, lumen. Bar = 100 μm.

arterial wall. The coronary arterial wall of a subject with KD who died with giant CAA showed positive staining for UTS2, UTS2R, and CD14 in infiltrating mononuclear inflammatory cells (**Figure 4**). This suggests a possible role for UTS2 and UTS2R involvement in the recruitment of CD14+ monocytes to the arterial wall, thus contributing to vessel wall inflammation. It is also possible that in KD, the CD14+ monocytes expressing UTS2 and UTS2R can differentiate into myofibroblasts, as has been reported in systemic sclerosis patients (24). Although plasma UTS2 levels did not correlate with coronary artery damage (data not shown), it is likely that the expression of UTS2 and the recruitment of cells occur in the tissues and not in the periphery. Our results raise the possibility that UTS2 and UTS2R could contribute to inflammation and CAA formation in KD through the induction of myofibroblast transformation in the vascular wall.

Myofibroblasts are spindle-shaped cells that appear after cardiac injury and contribute to cardiac remodeling (25). Myofibroblasts are formed through the process of epithelial-to-mesenchymal transition (EMT), in which cells of mesenchymal origin, such as fibroblasts, can differentiate into myofibroblasts. The process is triggered by multiple mediators including transforming growth factor (TGF)-β (26). Markers of myofibroblast phenotypic differentiation include expression of alpha-smooth muscle actin (αSMA), increased collagen synthesis, and enhanced cell migration (25). We have previously reported that myofibroblast-like cells and TGFβ have a role in aneurysm formation in those patients suffering from KD (4). Myofibroblast-like cells were found in the coronary arterial wall of KD patients and were shown to express IL-17, which recruits pro-inflammatory cells to the arterial wall to contribute to aneurysm formation and arterial damage. Studies by Zhang *et al.* demonstrated that UTS2 can induce increased TGFβ expression and secretion, αSMA expression, collagen synthesis, and cell migration in a time- and concentration-dependent manner in rat adventitial fibroblasts, suggesting that in rats, UTS2 and UTS2R can induce phenotypic differentiation of adventitial fibroblasts to myofibroblasts (27,28).

UTS2 may have a role in ongoing inflammation and persistent aneurysms in the convalescent stages of KD. In the present study, we showed that UTS2 and UTS2R were expressed in myofibroblast-like cells in both a coronary artery specimen 10 months post-KD (**Figure 4**) and an endarterectomy specimen with dense fibrotic regions with collagen deposition (**Figure 5**). Myofibroblasts have an important role in the development of aneurysms (4) and after formation of CAA, the aneurysmal arterial walls of patients with KD may remodel with activated myofibroblasts causing luminal narrowing and occlusion (29). UTS2R is a G-coupled protein receptor that, upon binding to UTS2, leads to downstream signaling that potentiates L-type calcium channels in cardiomyocytes (30). Genetic variation in calcium signaling pathways influences KD susceptibility and aneurysm formation (8). Investigating the role of UTS2 in calcium signaling through UTS2R may provide further insight into the role of UTS2 and UTS2R in KD pathogenesis. We recognize both strengths and limitations of the present study. This study draws a link between genetic risk factors for KD that serve as an eQTL for UTS2, and increased levels of this protein that may recruit inflammatory cells to the arterial wall and contribute to EMT, a process associated with aneurysm formation.

We recognize the descriptive nature of this study that should be viewed as hypothesis generating. Limitations include the small number of acute and convalescent paired transcriptome data available from subjects with CAA, making it difficult to determine whether persistence of elevated UTS2 levels in those with CAA during convalescence is due to persistent vascular wall inflammation or is an artifact of small sample size, the small number of KD autopsy tissues available for immunochemical studies, and the inability to genotype one of the tissue donors due to the poor quality of the DNA.

In summary, we demonstrated that polymorphisms in SLC8A1 influence the transcription of UTS2, with higher UTS2 transcript abundance and plasma protein levels observed in subjects with KD homozygous for SLC8A1 risk alleles. Both UTS2 and UTS2R were expressed in mononuclear inflammatory cells and spindle-shaped, myofibroblast-like cells in the coronary arterial wall of a subject with CAA and in spindle-shaped, myofibroblast-like cells in the femoral arterial wall of another subject with

peripheral aneurysms following KD. These data suggest that UTS2 and UTS2R may have a pro-inflammatory role associated with monocyte recruitment and myofibroblast generation that contributes to formation of CAA.

SUPPLEMENTARY MATERIAL

Supplementary material is linked to the online version of the paper at http://www.nature.com/pr

ACKNOWLEDGMENTS

We would like to thank Joan Pancheri, R.N. for clinical assistance, DeeAnna Scherrer for technical assistance, Denise Malicki, and Keith Rapp at Rady Children's Hospital San Diego for the kind gift of control tissues, Jennifer Santini at UCSD Neuroscience Microscopy Shared Facility for imaging support, and the parents who donated their children's samples for our studies.

AUTHOR CONTRIBUTIONS

J.C.B. and C.S. conceived the experiments; J.C.B., C.S., and C.Y.H. designed the experiments; C.Y.H. performed the experiments; C.Y.H. and C.S. analyzed the data; C.Y.H. wrote the manuscript; C.S. and J.C.B. revised the manuscript.

STATEMENT OF FINANCIAL SUPPORT

This work was funded in part by a grant from the Gordon and Marilyn Macklin Foundation in Bethesda, MD.

Disclosure: The authors declare no conflict of interest.

REFERENCES

1. Newburger JW, Takahashi M, Burns JC. Kawasaki disease. J Am Coll Cardiol 2016;67:1738–49.
2. Taubert KA, Rowley AH, Shulman ST. Nationwide survey of Kawasaki disease and acute rheumatic fever. J Pediatr 1991;119:279–82.
3. Gordon JB, Kahn AM, Burns JC. When children with Kawasaki disease grow up: myocardial and vascular complications in adulthood. J Am Coll Cardiol 2009;54:1911–20.
4. Shimizu C, Oharaseki T, Takahashi K, Kottek A, Franco A, Burns JC. The role of TGF-beta and myofibroblasts in the arteritis of Kawasaki disease. Hum Pathol 2013;44:189–98.
5. Lee AM, Shimizu C, Oharaseki T, et al. Role of TGF-beta signaling in remodeling of noncoronary artery aneurysms in Kawasaki disease. Pediatr Dev Pathol 2015;18:310–7.
6. Shimizu C, Sood A, Lau HD, et al. Cardiovascular pathology in 2 young adults with sudden, unexpected death due to coronary aneurysms from Kawasaki disease in childhood. Cardiovasc Pathol 2015;24:310–6.
7. Onouchi Y. Molecular genetics of Kawasaki disease. Pediatr Res 2009;65: 46 R–54 R.
8. Onouchi Y. Genetics of Kawasaki disease: what we know and don't know. Circ J 2012;76:1581–6.
9. Shimizu C, Eleftherohorinou H, Wright VJ, et al. Genetic variation in the SLC8A1 calcium signaling pathway is associated with susceptibility to kawasaki disease and coronary artery abnormalities. Circ Cardiovasc Genet 2016;9:559–68.
10. Ames RS, Sarau HM, Chambers JK, et al. Human urotensin-II is a potent vasoconstrictor and agonist for the orphan receptor GPR14. Nature 1999;401:282–6.
11. Ross B, McKendy K, Giaid A. Role of urotensin II in health and disease. Am J Physiol Regul Integr Comp Physiol 2010;298:R1156–72.
12. Zhang Y, Bao S, Kuang Z, Ma Y, Hu Y, Mao Y. Urotensin II promotes monocyte chemoattractant protein-1 expression in aortic adventitial fibroblasts of rat. Chin Med J 2014;127:1907–12.
13. Wong M, Silverman ED, Fish EN. Evidence for RANTES, monocyte chemotactic protein-1, and macrophage inflammatory protein-1 beta expression in Kawasaki disease. J Rheumatol 1997;24: 1179–85.
14. Terai M, Jibiki T, Harada A, et al. Dramatic decrease of circulating levels of monocyte chemoattractant protein-1 in Kawasaki disease after gamma globulin treatment. J Leukoc Biol 1999;65:566–72.
15. Segain JP, Rolli-Derkinderen M, Gervois N, Raingeard de la Bletiere D, Loirand G, Pacaud P. Urotensin II is a new chemotactic factor for UT receptor-expressing monocytes. J Immunol 2007;179:901–9.
16. Tran L, Kompa AR, Kemp W, Phrommintikul A, Wang BH, Krum H. Chronic urotensin-II infusion induces diastolic dysfunction and enhances collagen production in rats. Am J Physiol Heart Circ Physiol 2010;298: H608–13.
17. Zhao J, Ding W, Song N, et al. Urotensin II-induced collagen synthesis in cultured smooth muscle cells from rat aortic media and a possible involvement of transforming growth factor-beta1/Smad2/3 signaling pathway. Regul Pept 2013;182:53–8.
18. Numano F, Shimizu C, Jimenez-Fernandez S, et al. Galectin-3 is a marker of myocardial and vascular fibrosis in Kawasaki disease patients with giant aneurysms. Int J Cardiol 2015;201:429–37.
19. Hoang LT, Shimizu C, Ling L, et al. Global gene expression profiling identifies new therapeutic targets in acute Kawasaki disease. Genome Med 2014;6:541.
20. Asano T, Ogawa S. Expression of monocyte chemoattractant protein-1 in Kawasaki disease: the anti-inflammatory effect of gamma globulin therapy. Scand J Immunol 2000;51:98–103.
21. Brown TJ, Crawford SE, Cornwall ML, Garcia F, Shulman ST, Rowley AH. CD8 T lymphocytes and macrophages infiltrate coronary artery aneurysms in acute Kawasaki disease. J Infect Dis 2001;184:940–3.
22. Katayama K, Matsubara T, Fujiwara M, Koga M, Furukawa S. CD14 +CD16+ monocyte subpopulation in Kawasaki disease. Clin Exp Immunol 2000;121:566–70.
23. Wong KL, Tai JJ, Wong WC, et al. Gene expression profiling reveals the defining features of the classical, intermediate, and nonclassical human monocyte subsets. Blood 2011;118:e16–31.
24. Binai N, O'Reilly S, Griffiths B, van Laar JM, Hugle T. Differentiation potential of CD14+ monocytes into myofibroblasts in patients with systemic sclerosis. PLoS One 2012;7:e33508.
25. Baum J, Duffy HS. Fibroblasts and myofibroblasts: what are we talking about? J Cardiovasc Pharmacol 2011;57:376–9.
26. Zavadil J, Bottinger EP. TGF-beta and epithelial-to-mesenchymal transitions. Oncogene 2005;24:5764–74.
27. Zhang YG, Li J, Li YG, Wei RH. Urotensin II induces phenotypic differentiation, migration, and collagen synthesis of adventitial fibroblasts from rat aorta. J Hypertens 2008;26:1119–26.
28. Zhang YG, Hu YC, Mao YY, et al. Transforming growth factor-beta1 involved in urotensin II-induced phenotypic differentiation of adventitial fibroblasts from rat aorta. Chin Med J 2010;123:3634–9.
29. Orenstein JM, Shulman ST, Fox LM, et al. Three linked vasculopathic processes characterize kawasaki disease: a light and transmission electron microscopic study. PloS one 2012;7:e38998.
30. Zhang Y, Ying J, Jiang D, et al. Urotensin-II receptor stimulation of cardiac L-type Ca2+ channels requires the betagamma subunits of Gi/o-protein and phosphatidylinositol 3-kinase-dependent protein kinase C beta1 isoform. J Biol Chem 2015;290:8644–55.